Highly Efficient Regulation Strategy of Fluorescence Emission Wavelength via Designing the Structure of Carbon Dots

haiyan bai
Xi'an Technological University
Xilang Jin
Xi'an Technological University
Zhao Cheng
Xi'an Medical University
Hongwei Zhou
Xi'an Technological University
Haozhe Wang
Xi'an Technological University
Jiajia Yu
Xi'an Technological University
Jialing Zuo
Xi'an Technological University
Weixing Chen (chenwx@xatu.edu.cn)
Xi'an Technological University

Research Article

Keywords: regulation strategy, multicolor CDs, DFT theoretical calculation, sp2 conjugated domain, LED

Posted Date: December 2nd, 2022

DOI: https://doi.org/10.21203/rs.3.rs-2242391/v1

Abstract

Multicolor carbon dots (CDs) possess tremendous potential applications, especially in optoelectronic devices. However, further applications of multi-color LED have been constrained due to the very limited researches concerning the wavelength control mechanism of multi-color CDs. In this work, through theoretical calculation and experimental verification, the regulatory effects of sp^2 conjugated domain on the fluorescence wavelength of CDs were explored. Firstly, through a regulation on the structure size and the introduction of amide bonds, four kinds of structures were designed in DFT theoretical calculation to explore the influence of sp^2 conjugated domain on the fluorescence wavelength of CDs theoretically. Then, using thiourea and *p*-phenylenediamine as the precursors and by regulating the reaction solvents, multicolor CDs with blue, green and red fluorescence emission were prepared to experimentally verify the emission mechanism. It was confirmed that the increasing structure size and the introduction of amide bond would induce an increasing size of the sp^2 conjugated domain, leading to the red shift of the CDs fluorescence wavelength. Finally, in order to suppress the self-quenching performance, the CDs@PVP fluorescent film possessing bright solid-state fluorescence was constructed for a better application in light-emitting diodes. The approach provided an effective strategy to realize the programmed regulation on the fluorescence wavelength of CDs, offering us full of potentials for the applications of CDs in the photoelectric device fields.

1. Introduction

Carbon dots (CDs), as a new type of zero-dimensional materials with fluorescence luminescence properties {Zhao, 2022}, have been widely used in biological imaging {Ayiloor Rajesh, 2022}; {Ding, 2018}; {Jiang, 2020}; {Lin, 2022}, fluorescence sensing {Li, 2021}; {Pu, 2021}; {Zheng, 2020}, especially in light-emitting diodes based on their facile synthesis, environmental stability, low toxicity {Dai, 2022}; {Geng, 2022}; {Li, 2022}; {Liu, 2021}, excellent biocompatibility and photoelectric performance {Jin, 2020}; {Li, 2020}; {Rad, 2021}; {Wang, 2021}. As the core of the new generation of solid-state lighting {Choi, 2015}; {Pattison, 2018}, CDs based LED has the following advantages compared with other lighting display devices: (1) high luminous efficiency {Jang, 2020}, (2) long service life, safety and reliability, known as the "fourth generation lighting source" {Dai, 2014}; {Zhao and Tan 2021} ; (3) small and easy to package {Li, 2020}; {Pu, 2020}. Multicolor CDs have great application potentials in multi-color LEDs due to their controllable wavelength. However, further applications of multi-color LED have been constrained due to the very limited researches concerning the wavelength control mechanism of multi-color CDs.

In recent years, researchers have proposed a variety of synthetic routes or reaction methods to satisfy CDs' emission {Ji, 2022}; {Li, 2022}; {Qu, 2022}; {Xu, 2022}; {Yu, 2021}; {Zhang, 2022}. Kwon and his coworkers {Kwon, 2014} have reported a synthetic method and prepared a range of the GQDs (Graphite phase quantum dots) with certain size distributions via amidative cutting of tattered graphite, which could achieve a size range of 2 to over 10 nm for GQDs by simply regulating the amine concentration. Accompanied with the increasing size was the narrowed down energy gaps in the synthesized GQDs, leading to a red shift of the CDs with colorful photoluminescence from blue to brown. Jin {Jin 2020}

developed a green hydrothermal method to obtain three emission colors of CDs using l-tyrosine (for blue CDs), *o*-phenylendiamine (for green CDs) and l-tyrosine/*o*-phenylendiamine mixture (for orange-red CDs), which also proved the dependence of CDs PL properties on their surface group and the exciton-trapping functions of the surface functional groups. However, the regulation mechanism on the emission wavelength of CDs still needs to be verified through theoretical calculations and related experiments.

In this work, through theoretical and experimental verifications, the regulatory effects of sp^2 conjugated domain on the fluorescence wavelength of CDs were explored. Firstly, by changing the structural size and introducing amide groups in DFT theoretical calculation, four kinds of CDs structures were designed to investigate the structural effect of sp^2 conjugated domain on wavelength regulation theoretically. Secondly, with thiourea and *p*-phenylenediamine as the precursors, multicolor CDs emitting blue, green and red fluorescence were prepared by regulating the reaction solvents. The analysis results confirmed that the increasing structure size and the introduction of amide groups would induce an increase of sp^2 conjugated domain, leading to the red shift of the CDs fluorescence wavelength. Finally, the obtained multicolor CDs were applied for LED device in the form of CDs@PVP films. The schematic illustration of multicolor CDs is shown in Fig. 1.

2. Experimental

Materials and measurements were shown in SI.

2.1 DFT Simulation calculation

The ground state geometry is optimized using DFT, and the excited states are calculated with linear response time-dependent DFT (TD-DFT) at the optimized ground state geometry. All calculations are performed with the Gaussian 16 package (Rev. C.01) using the CAM-B3LYP functional and the 6-311G* basis set. Grimme's D3BJ dispersion correction was used to improve the calculation accuracy.

2.2 Synthesis of CDs

The d-CDs were obtained via a facile one-step hydrothermal strategy. 0.1 g thiourea and 0.1 g *p*-phenylenediamine were dissolved in 10 mL DMF, then the mixture was dispersed by ultrasonic unit for 5 min. The obtained uniform solution was sealed in a Teflon autoclave and heated at 200 ℃ for 8 h. After that, the suspension was filtered by a 0.22 μm pore diameter microporous membrane. The purified solution was freeze-dried to obtain solid-state CDs.

The synthetic method of e-CDs and m-CDs was similar, except that the reaction solvents were changed to ethanol and methanol, respectively. In addition, to further verify the effect of sp^2 conjugated domain on the fluorescence wavelength of CDs, two kinds of CDs were prepared with the same process except that the reaction solvents were changed to formamide (f-CDs) and DMA(a-CDs).

2.3 Preparation of CDs@PVP fluorescent film

1g PVP was dissolved in 20 mL filtered CDs solution, coated on the template after stirred evenly, then solidified at room temperature for 24 h. Finally, the blue, green, and red emissive CDs@PVP films under 365 nm excitation light were obtained, respectively.

3. Results And Discussion

3.1 Structure design and DFT theoretical calculation

In order to investigate the mechanism of CDs wavelength regulation, by changing the structural size and by introducing amide groups in the DFT theoretical calculation, four CDs structures were designed to explore the effect of sp^2 conjugated domain size on the wavelength regulation theoretically {Zhang, 2022}. As shown in Fig. 2a, the basic structure from 1 to 3, except the structural size, was similar, which could effectively verify the effect of structural size on the fluorescence wavelength of CDs. Furthermore, when the -OH group on the surface of structure 3 was replaced by -CONH- to give structure 4, the effect of amide groups on the fluorescence wavelength of CDs could be verified. These structures could be used to explore the influence of sp^2 conjugated domain on the HOMO-LUMO energy gap of CDs.

DFT theoretical calculations were carried out for HOMO-LUMO energy level of the four mentioned structures. Detailed calculation process was described in section 2.1 {Grimme, 2011}; {Yanai, 2004}. From structure 1 to structure 3, in Fig. 2b, a trend of gradual decrease in turns (6.18 ev, 4.92 ev, 4.30 ev) in the energy gap was depicted, which indicated that the increase of the structural size could lead to a red shift fluorescence wavelength of CDs (The decrease of the energy gap would lead to the red shift of the CDs fluorescence wavelength) {Tang, 2022}. In Fig. 2c, the energy level gap of structure 3 and structure 4 was 4.30 ev and 4.28 ev, respectively, which indicated that the introduction of amide groups could induce the red shift fluorescence wavelength. Through two measures in theoretical calculation, it was improved that the increasing size of sp^2 conjugated domain could lead to the red shift of CDs fluorescence wavelength.

3.2 Synthesis, basic morphology and structure

Based on the results of DFT theoretical calculation, the effect of sp^2 conjugated domain on the emission wavelength of CDs was expected to be further testified in the experiments. Thiourea and *p*-phenylenediamine were selected as precursors, three kinds of CDs, emitting red (d-CDs), green (e-CDs), blue (m-CDs), were successfully synthesized by one-step hydrothermal reaction with DMF, ethanol and methanol as the reaction solvents, respectively. In order to optimize the experimental conditions, CDs were synthesized at 160 ℃, 180 ℃, 200 ℃ and 220 ℃ in each reaction solvent. Accompanied with the increasing reaction temperature, it could be seen that the fluorescence intensity firstly increased and then decreased (Fig. S1a). When the reaction temperature was 200 ℃, the fluorescence intensity was the highest. In order to explore the optimal reaction time, CDs were synthesized under the reaction time of 3 h, 5 h, 8 h, 10 h and 12 h, respectively. When reaction time was extended, the fluorescence intensity showed a trend of firstly increasing and then decreasing (Fig. S1b) and reached the highest fluorescence intensity at 8 h. Based on this inquiry, the reaction conditions were optimized as follows: thiourea and *p*-

phenylenediamine were reacted in methanol, ethanol and DMF for 8 h at 200 ℃, respectively. The quantum yield of these CDs was tested to be 21.1%(m-CDs), 16.5%(e-CDs), 8.3%(d-CDs), respectively. And the pH stability, salt resistance and UV absorption of CDs were described in Fig. S1c, Fig. S1d, Fig. S1e, which combined to indicate that the synthesized CDs presented remarkable conjugate structure (UV absorption) and had excellent stability in various environments.

For a better demonstration of the CDs structural size, TEM, XRD and Raman spectra were carried out. As seen in the TEM images (Fig. 3a–Fig. 3c), all three kinds of CDs presented uniform distribution of morphology and size. The average size of the synthesized CDs was 7.068 nm (d-CDs), 6.098 nm (e-CDs) and 3.451 nm (m-CDs) (Fig. 3d–Fig. 3f). Considering that the CDs emitting red, green and blue in turns, it could be concluded that the fluorescence wavelength red shifts took place with the particle size increasing, which was probably caused by the increased size of sp^2 conjugated domain. The XRD test was carried out to verify whether the CDs have obvious conjugated structures (Fig. 3g). The peak positions located at 22°, 24° and 25° for the three kinds of CDs belonged to (002) crystal plane of graphite phase carbon. This indicated that the three kinds of CDs had obvious conjugated structures {Zhang 2022}. The Raman spectra of the three CDs were presented in Fig. 3h. All the three kinds of CDs showed obvious D-band (1353cm^{-1}) and G-band (1561cm^{-1}). The I_G/I_D of d-CDs, e-CDs, m-CDs was 1.1, 1.03 and 0.88, respectively, which confirmed that the order of the decreased size of the sp^2 conjugated domain was d-CDs, e-CDs, m-CDs {Bai, 2021} .

In order to explore the surface groups of the three kinds of CDs, Zeta potential, Fourier transform infrared spectroscopy (FT-IR) and X-ray photoelectron spectroscopy (XPS) were carried out. The Zeta potential results were shown in Fig. 3i, these CDs showed obvious peak at -15.5 mV, -16.1 mV, -23.2 mV. It was revealed that the surface states of the three CDs were different. From the FTIR spectra shown in Fig. 4a, these CDs had the same peaks at 820 cm^{-1}, 1395 cm^{-1}, 1500 cm^{-1} and 3127 cm^{-1}. Specifically, 820 cm^{-1} was the characteristic peak of p-disubstituted benzene, 1395 cm^{-1} and 1500 cm^{-1} could be attributed to the characteristic absorption peaks of C = S and C = C. And 3127cm^{-1} could be regarded as the stretching vibration of N-H. The characteristic vibration peak of d-CDs was at 1620 cm^{-1}, related to the stretching vibration caused by C = O of amide, which was not found in m-CDs and e-CDs. Therefore, it could be speculated that, amide groups were successfully introduced into the structure of d-CDs.

The full spectrum specific results of XPS were shown in Fig. 4b. The peaks of the four constituent elements C1s, N1s, O1s and S2p were observed at about ~ 284.18 eV, ~ 398.93 eV, ~ 531.81 eV and ~ 162.23 eV for the CDs (The specific peaks of the three CDs were shown in Tab S1), respectively {Sun, 2020}. In the high-resolution XPS spectra of C1s, four types of carbon signals at about 284.0 eV, 284.4 eV, 285.3 eV and 287.4 eV could be found in the high-resolution C1s for d-CDs (Fig. 4c), which was in corresponding with C = C/C-C, C-O, C-N and -CONH- bonds, respectively. There were three types of carbon signals at 283.7 eV, 284.4 eV and 285.3 eV for e-CDs and m-CDs (Fig. 4d, Fig. 4e), corresponding to C = N, C-O and C-N bonds respectively. The XPS results proved that amide groups were successfully introduced into the structure of d-CDs.

Moreover, the contents of C = C/C = N in the three kinds of CDs were 31.25% (m-CDs), 37.11% (e-CDs) and 46.84% (d-CDs), respectively (Table 1). N1s spectra of the fluorescent CDs simulated three characteristic peaks at 397.5 eV, 398.8 eV and 400.0 eV, which were corresponded to pyridine type N, graphite type N and pyrrole type N respectively (Fig. S2, Fig. S3, Fig. S4). The content of graphite type N was 32.01% (m-CDs), 45.99% (e-CDs) and 49.83% (d-CDs). It was showed that the sp^2 conjugated domain was increasing in turns, which furtherly proved the connections of amide group introduction and the increasing size of sp^2 conjugated domain (Table 1).

Table 1
Element content of the CDs

	C(%)	N(%)	O(%)	S(%)	sp^2 C domain	sp^2 N domain	-CONH-
					C = C/C = N(%)	Graphitic N(%)	-CONH-(%)
D-CDs	76.27	13.12	8.26	2.35	46.84	49.83	5.94
e-CDs	74.17	7.96	16.37	1.49	37.11	45.99	0
m-CDs	72.35	18.04	5.39	4.23	1.25	32.01	0

3.3 Fluorescence properties of CDs

CDs emitting red (d-CDs, Em = 620 nm), green (e-CDs, Em = 520 nm), (m-CDs, Em = 445 nm) were presented at Fig. 4f. Excitation-emission maps of m-CDs, e-CDs, and d-CDs were shown in Fig. 5a, Fig. 5b, Fig. 5c. The m-CDs exhibited multiple luminescence centers covering from 400 nm to 480 nm, with the main emission center in blue region at 445 nm (Fig. 5a). The e-CDs exhibited a main green emission center at 520 nm (Fig. 5b). The d-CDs exhibited multiple luminescence centers covering from 605 nm to 635 nm, with the main emission center in red region at 620 nm (Fig. 5c). Combined with the above analyses, it could be proved that the increasing size of sp^2 conjugated domain could induce a red shift of the fluorescence wavelength.

In order to further verify the above-mentioned mechanism, another two kinds of CDs (f-CDs, a-CDs) were prepared using thiourea and *p*-phenylenediamine as the precursors and formamide/DMA as the reaction solvents. The normalized fluorescence emission diagram was shown in Fig. 5d. In a comparison of the m-CDs and f-CDs, amide group was introduced in f-CDs, the fluorescence wavelength of f-CDs increased from 445 nm to 605 nm, which proved that the introduction of amide group on CDs could lead to the red shift of CDs fluorescence wavelength. As for the d-CDs and a-CDs, the size of sp^2 conjugated domain in d-CDs was enlarged (Fig. S5), and the fluorescence emission wavelength was increased from 620 nm to 650 nm. It could be verified again that the enlarged size of sp^2 conjugated domain could cause the red shift of the fluorescence wavelength of CDs.

3.4 Luminescent properties of LEDs based on CDs@PVP fluorescent films

The aggregation quenching effect of CDs, caused by direct π - π interaction or excessive resonance energy transfer, may seriously limit the further application of CDs. To avoid this phenomenon, CDs was doped into PVP (Polyvinylpyrrolidone) to suppress the aggregation induced luminescence quenching. The abundant surface chains of PVP could be able to prevent the graphitizing cores from π - π interactions. Thus, the CDs particles embedded in the PVP kept an appropriate distance from each other, which effectively avoided the consequent fluorescence quenching of solid-state CDs. For a better application in LED devices, CDs@PVP fluorescent films were prepared, as shown in Fig. 6.

The CDs@PVP fluorescent film under the irradiation of 365nm ultraviolet lamp was shown in the Fig. 6a-Fig. 6c. The bright blue, green and red fluorescence could be observed with naked eyes under the irradiation of 365 UV lamp, which indicated that aggregation quenching effect could be effectively suppressed. Furthermore, The CDs@PVP solution was uniformly coated on commercial UV chips (365 nm) to prepare multicolor CDs@PVP based LED. The corresponding CIE color coordinates of the CDs@PVP based LEDs (m-CDs@PVP in (0.17, 0.14), e-CDs@PVP in (0.36, 0.51), d-CDs@PVP in (0.59, 0. 4)) were described in Fig. 6d- Fig. 6f. The results indicated that the synthesized CDs could be used in multicolor LED and would have excellent development in the field of photoluminescence.

4. Conclusions

In summary, through DFT theoretical calculation and experiments, it was found that the size of sp^2 conjugated domain could regulate the wavelength of CDs. Meanwhile, multicolor CDs (emitting red (620 nm), green (520 nm), and blue (445 nm) fluorescence) with the designed structures, in accordance with the DFT theoretical calculation results, were successfully prepared by the hydrothermal reaction. The CDs@PVP solid-state fluorescent films could be furtherly applied to multicolor LEDs. The approach provided an effective and novel strategy to realize the programmed regulation on the fluorescence wavelength of CDs, offering us full of potentials for the applications of CDs in the photoelectric device fields.

Declarations

Fundings

This work was financially supported by the National Natural Science Foundation of China (No. 21807085), the Innovative Talents Promotion Plan-Young Science and Technology Star Project (No. 2022KJXX-88) and Technology Innovation Leading Program of Shaanxi (No. 2020QFY07-05).

Competing Interests

The authors declare no competing financial interest.

Authors' Contributions

Haiyan Bai: Methodology, Investigation, writing - Original Draft. Xilang Jin: Supervision, project administration and writing - review & editing. Zhao Cheng: Methodology, Data curation. Hongwei Zhou: Methodology, Data curation. Haozhe Wang: Data curation, Formal analysis. Jiajia Yu: Methodology, Investigation. Jialing Zuo: Methodology, Data curation. Weixing Chen: Supervision, Validation, Methodology.

Supplementary data

Supplementary data associated with this article can be found, at the document of Supplementary information.

References

1. Ayiloor Rajesh G, John V L, Pookunnath Santhosh A, Krishnan Nair Ambika A, Thavarool Puthiyedath V, (2022) Carbon Dots from Natural Sources for Biomedical Applications. Particle & Particle Systems Characterization 39 (9):2200017.https://onlinelibrary.wiley.com/doi/abs/10.1002/ppsc.202200017
2. Bai H, Chen W, Yang J, Cao Y, Yu J, Zhao H, Zhou H, Jin X, (2021) Green synthesis of orange emissive carbon dots for the detection of Ag(+)and their application via solid-phase sensing and security ink. Nanotechnology 33 (3):035709.https://www.ncbi.nlm.nih.gov/pubmed/34638108
3. Choi M K, Yang J, Kang K, Kim D C, Choi C, Park C, Kim S J, Chae S I, Kim T-H, Kim J H, Hyeon T, Kim D-H, (2015) Wearable red–green–blue quantum dot light-emitting diode array using high-resolution intaglio transfer printing. Nature Communications 6 (1):7149.https://doi.org/10.1038/ncomms8149
4. Dai R, Chen X, Ouyang N, Hu Y, (2022) A pH-controlled synthetic route to violet, green, and orange fluorescent carbon dots for multicolor light-emitting diodes. Chemical Engineering Journal 431 134172.https://www.sciencedirect.com/science/article/abs/pii/S1385894721057454
5. Dai X, Zhang Z, Jin Y, Niu Y, Cao H, Liang X, Chen L, Wang J, Peng X, (2014) Solution-processed, high-performance light-emitting diodes based on quantum dots. Nature 515 96–99.https://www.nature.com/articles/nature13829
6. Ding H, Wei J S, Zhang P, Zhou Z Y, Gao Q Y, Xiong H M, (2018) Solvent-Controlled Synthesis of Highly Luminescent Carbon Dots with a Wide Color Gamut and Narrowed Emission Peak Widths. Small 14 (22):e1800612.https://www.ncbi.nlm.nih.gov/pubmed/29709104
7. Geng B, Hu J, Li Y, Feng S, Pan D, Feng L, Shen L, (2022) Near-infrared phosphorescent carbon dots for sonodynamic precision tumor therapy. Nature Communications 13 (1):5735.https://doi.org/10.1038/s41467-022-33474-8
8. Grimme S, Ehrlich S, Goerigk L, (2011) Effect of the damping function in dispersion corrected density functional theory. Journal of Computational Chemistry 32 (7):1456–1465.https://doi.org/10.1002/jcc.21759
9. Jang E, Kim Y, Won Y-H, Jang H, Choi S-M, (2020) Environmentally Friendly InP-Based Quantum Dots for Efficient Wide Color Gamut Displays. ACS Energy Letters 5 1316–

1327.https://pubs.acs.org/doi/10.1021/acsenergylett.9b02851

10. Ji C, Han Q, Zhou Y, Wu J, Shi W, Gao L, Leblanc R M, Peng Z, (2022) Phenylenediamine-derived near infrared carbon dots: The kilogram-scale preparation, formation process, photoluminescence tuning mechanism and application as red phosphors. Carbon 192 198–208.https://www.sciencedirect.com/science/article/pii/S0008622322001397
11. Jiang L, Ding H, Xu M, Hu X, Li S, Zhang M, Zhang Q, Wang Q, Lu S, Tian Y, Bi H, (2020) UV-Vis-NIR Full-Range Responsive Carbon Dots with Large Multiphoton Absorption Cross Sections and Deep-Red Fluorescence at Nucleoli and In Vivo. Small 16 (19):e2000680.https://www.ncbi.nlm.nih.gov/pubmed/32285624
12. Jin L, Zhang L, Yang L, Wu X, Zhang C, Wei K, He L, Han X, Qiao H, Asiri A M, Alamry K A, Zhang K, (2020) Orange-red, green, and blue fluorescence carbon dots for white light emitting diodes. Journal of Materials Science & Technology 50 184–191.https://doi.org/10.1016/j.jmst.2020.03.020
13. Kwon W, Kim Y H, Lee C L, Lee M, Choi H C, Lee T W, Rhee S W, (2014) Electroluminescence from graphene quantum dots prepared by amidative cutting of tattered graphite. Nano Lett 14 (3):1306–1311.https://www.ncbi.nlm.nih.gov/pubmed/24490804
14. Li M, Yang M, Liu B, Guo H, Wang H, Li X, Wang L, James T D, (2022) Self-assembling fluorescent hydrogel for highly efficient water purification and photothermal conversion. Chemical Engineering Journal 431 134245.https://www.sciencedirect.com/science/article/abs/pii/S1385894721058186
15. Li N, Meng T, Ma L, Zhang H, Yao J, Xu M, Li C M, Jiang J, (2020) Curtailing Carbon Usage with Addition of Functionalized $NiFe_2O_4$ Quantum Dots: Toward More Practical S Cathodes for Li–S Cells. Nano-Micro Letters 12 (1):145.https://doi.org/10.1007/s40820-020-00484-4
16. Li P, Sun L, Xue S, Qu D, An L, Wang X, Sun Z, (2022) Recent advances of carbon dots as new antimicrobial agents. SmartMat 3 (2):226–248.https://onlinelibrary.wiley.com/doi/abs/10.1002/smm2.1131
17. Li Q, Bai Z, Xi X, Guo Z, Liu C, Liu X, Zhao X, Li Z, Cheng Y, Wei Y, (2021) Rapid microwave-assisted green synthesis of guanine-derived carbon dots for highly selective detection of Ag(+) in aqueous solution. Spectrochim Acta A Mol Biomol Spectrosc 248 119208.https://www.ncbi.nlm.nih.gov/pubmed/33257251
18. Li X, Lin Q, Song J, Shen H, Zhang H, Li L S, Li X, Du Z, (2020) Quantum-Dot Light-Emitting Diodes for Outdoor Displays with High Stability at High Brightness. Advanced Optical Materials 8 (2):1901145.https://onlinelibrary.wiley.com/doi/abs/10.1002/adom.201901145
19. Lin F, Jia C, Wu F-G, (2022) Carbon Dots for Intracellular Sensing. Small Structures 3 (9):2200033.https://onlinelibrary.wiley.com/doi/abs/10.1002/sstr.202200033
20. Liu G, Kong D, Han J, Zhou R, Gao Y, Wu Z, Zhao L, Wang C, Wang L, Lu G, (2021) Solvent-controlled synthesis of full-color carbon dots and its application as a fluorescent food-tasting sensor for specific recognition of jujube species. Sensors and Actuators B: Chemical 342 129963.https://www.sciencedirect.com/science/article/pii/S0925400521005323

21. Pattison P M, Tsao J Y, Brainard G C, Bugbee B, (2018) LEDs for photons, physiology and food. Nature 563 (7732):493–500.https://doi.org/10.1038/s41586-018-0706-x
22. Pu C, Dai X, Shu Y, Zhu M, Peng X, (2020) Electrochemically-stable ligands bridge photoluminescence-electroluminescence gap of quantum dots. Nature Communications 11 937.https://www.nature.com/articles/s41467-020-14756-5
23. Pu J, Liu C, Wang B, Liu P, Jin Y, Chen J, (2021) Orange red-emitting carbon dots for enhanced colorimetric detection of Fe(3). Analyst 146 (3):1032–1039.https://www.ncbi.nlm.nih.gov/pubmed/33300891
24. Qu Y, Bai X, Li D, Zhang X, Liang C, Zheng W, Qu S, (2022) Solution-processable carbon dots with efficient solid-state red/near-infrared emission. J Colloid Interface Sci 613 547–553.https://www.ncbi.nlm.nih.gov/pubmed/35063786
25. Rad R R, Gualdrón-Reyes A F, Masi S, Ganji B A, Taghavinia N, Gené-Marimon S, Palomares E, Mora-Seró I, (2021) Tunable Carbon–CsPbI3 Quantum Dots for White LEDs. Advanced Optical Materials 9 (4):2001508.https://onlinelibrary.wiley.com/doi/abs/10.1002/adom.202001508
26. Sun M, Han Y, Yuan X, Jing P, Zhang L, Zhao J, Zheng Y, (2020) Efficient full-color emitting carbon-dot-based composite phosphors by chemical dispersion. Nanoscale 12 (29):15823–15831.https://www.ncbi.nlm.nih.gov/pubmed/32692328
27. Tang S, Chen D, Yang Y, Wang C, Li X, Wang Y, Gu C, Cao Z, (2022) Mechanisms behind multicolor tunable Near-Infrared triple emission in graphene quantum dots and ratio fluorescent probe for water detection. J Colloid Interface Sci 617 182–192.https://www.ncbi.nlm.nih.gov/pubmed/35276519
28. Wang X, Ma Y, Wu Q, Wang Z, Tao Y, Zhao Y, Wang B, Cao J, Wang H, Gu X, Huang H, Li S, Wang X, Hu F, Shao M, Liao L, Sham T-K, Liu Y, Kang Z, (2021) Ultra-Bright and Stable Pure Blue Light-Emitting Diode from O, N Co-Doped Carbon Dots. Laser & Photonics Reviews 15 (3):2000412.https://onlinelibrary.wiley.com/doi/abs/10.1002/lpor.202000412
29. Xu J, Liang Q, Li Z, Osipov V Y, Lin Y, Ge B, Xu Q, Zhu J, Bi H, (2022) Rational Synthesis of Solid-State Ultraviolet B Emitting Carbon Dots via Acetic Acid-Promoted Fractions of sp(3) Bonding Strategy. Adv Mater 34 (17):e2200011.https://www.ncbi.nlm.nih.gov/pubmed/35246877
30. Yanai T, Tew D P, Handy N C, (2004) A new hybrid exchange-correlation functional using the Coulomb-attenuating method (CAM-B3LYP). Chemical Physics Letters 393 (1–3):51–57.https://doi.org/10.1016/j.cplett.2004.06.011
31. Yu Y, Wang X, Jia X, Feng Z, Zhang L, Li H, He J, Shen G, Ding X, (2021) Aptamer Probes Labeled with Lanthanide-Doped Carbon Nanodots Permit Dual-Modal Fluorescence and Mass Cytometric Imaging. Advanced Science 8 (24):e2102812.https://www.ncbi.nlm.nih.gov/pubmed/34719883
32. Zhang B, Wang B, Ushakova E V, He B, Xing G, Tang Z, Rogach A L, Qu S, (2022) Assignment of Core and Surface States in Multicolor-Emissive Carbon Dots. Small e2204158.https://www.ncbi.nlm.nih.gov/pubmed/36216592
33. Zhang X Y, Li Y, Wang Y Y, Liu X Y, Jiang F L, Liu Y, Jiang P, (2022) Nitrogen and sulfur co-doped carbon dots with bright fluorescence for intracellular detection of iron ion and thiol. J Colloid

Interface Sci 611 255–264.https://www.ncbi.nlm.nih.gov/pubmed/34953458

34. Zhao B, Ma H, Zheng M, Xu K, Zou C, Qu S, Tan Z A, (2022) Narrow-bandwidth emissive carbon dots: A rising star in the fluorescent material family. Carbon Energy 4 (1):88–114.https://doi.org/10.1002/cey2.175
35. Zhao B, Tan Z A, (2021) Fluorescent Carbon Dots: Fantastic Electroluminescent Materials for Light-Emitting Diodes. Advanced Science 8 (7):2001977.https://onlinelibrary.wiley.com/doi/abs/10.1002/advs.202001977
36. Zheng S, Li D, Fodjo E K, Deng W, (2020) Colorimetric/fluorescent/SERS triple-channel sensing of Cu^{2+} in real systems based on chelation-triggered self-aggregation. Chemical Engineering Journal 399 125840.https://www.sciencedirect.com/science/article/abs/pii/S1385894720319689

Figures

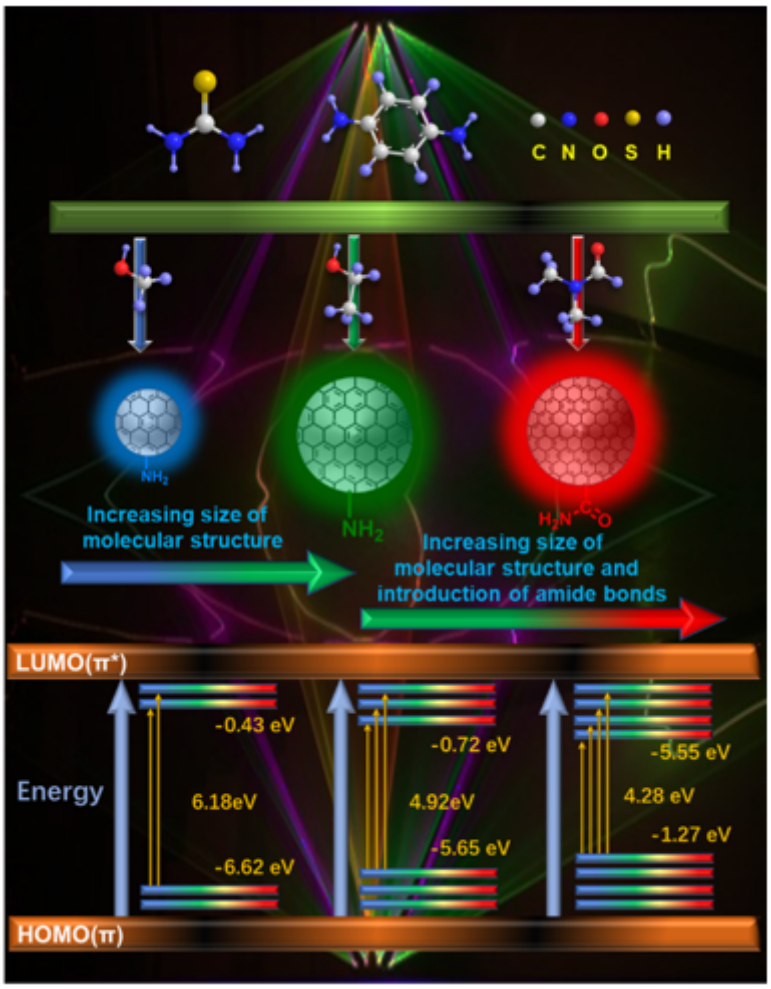

Figure 1

Schematic illustration of multicolor CDs.

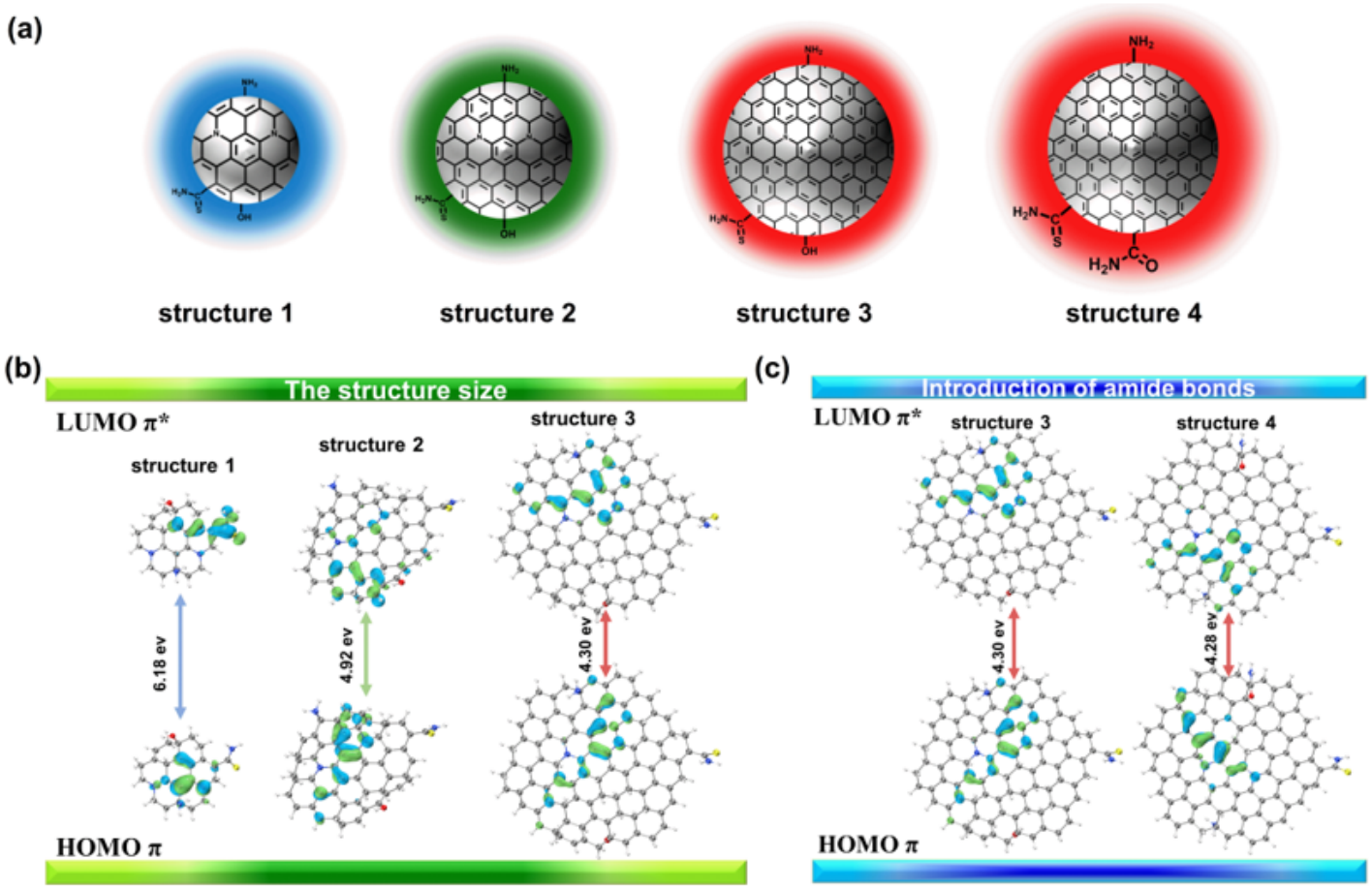

Figure 2

(a) The scheme of four kinds of designed structures; **(b) (c)** DFT theoretical calculation of the designed four kinds of structures.

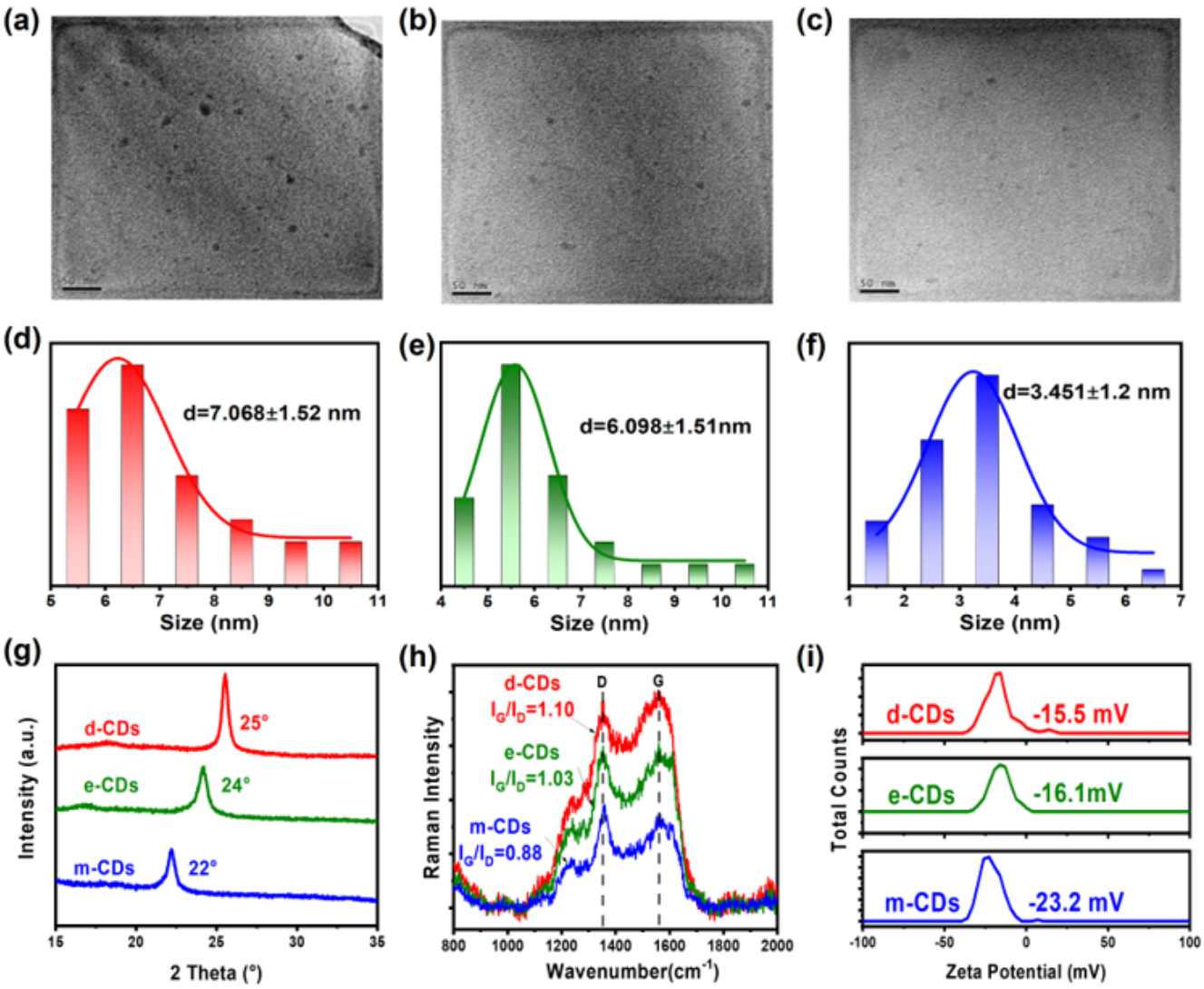

Figure 3

TEM of **(a)** d-CDs **(b)** e-CDs **(c)**m-CDs, size distribution diagram of **(d)** d-CDs **(e)** e-CDs **(f)**m-CDs, **(g)** XRD **(h)** Raman **(i)** Zeta potential of the CDs.

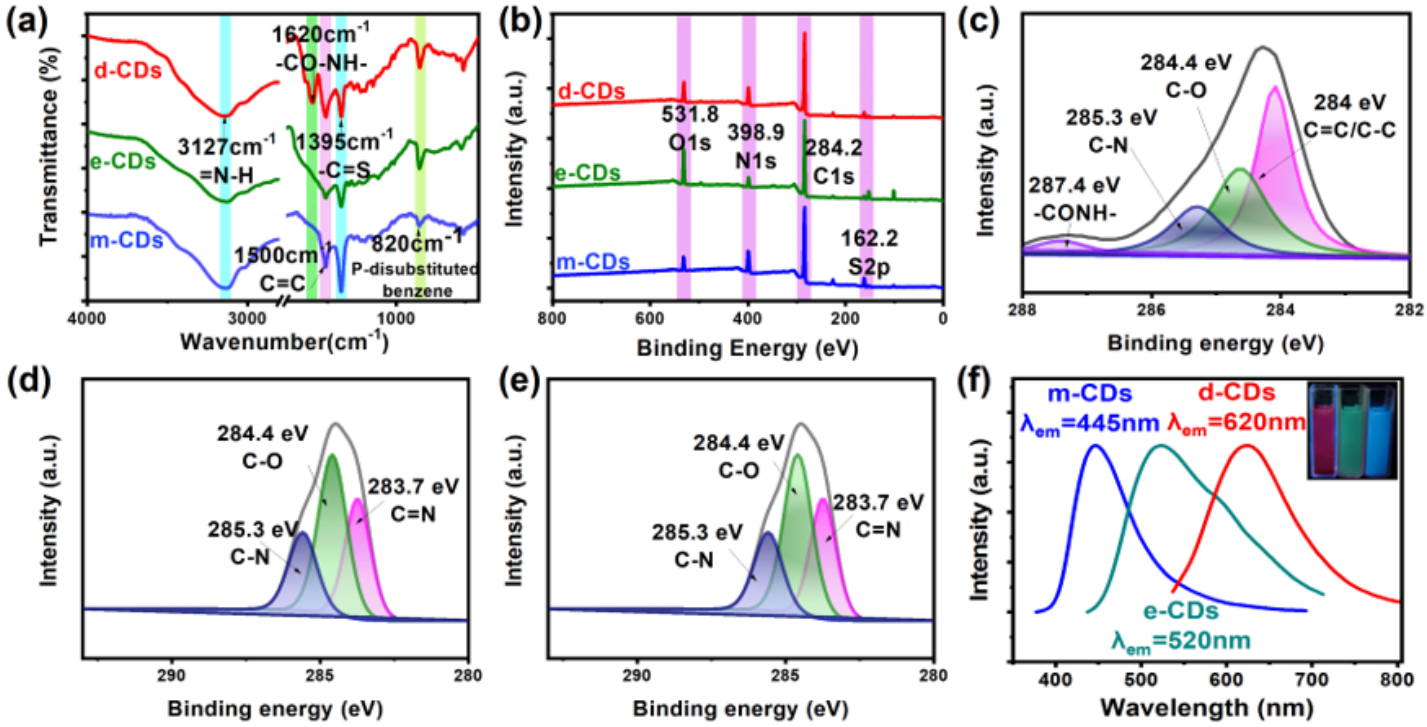

Figure 4

(a) FT-IR, **(b)**XPS survey, High-resolution C1s spectra of **(c)** d-CDs **(d)**e-CDs **(e)** m-CDs, **(f)** The corresponding normalized maximum emission spectra of m-CDs, e-CDs, d-CDs.

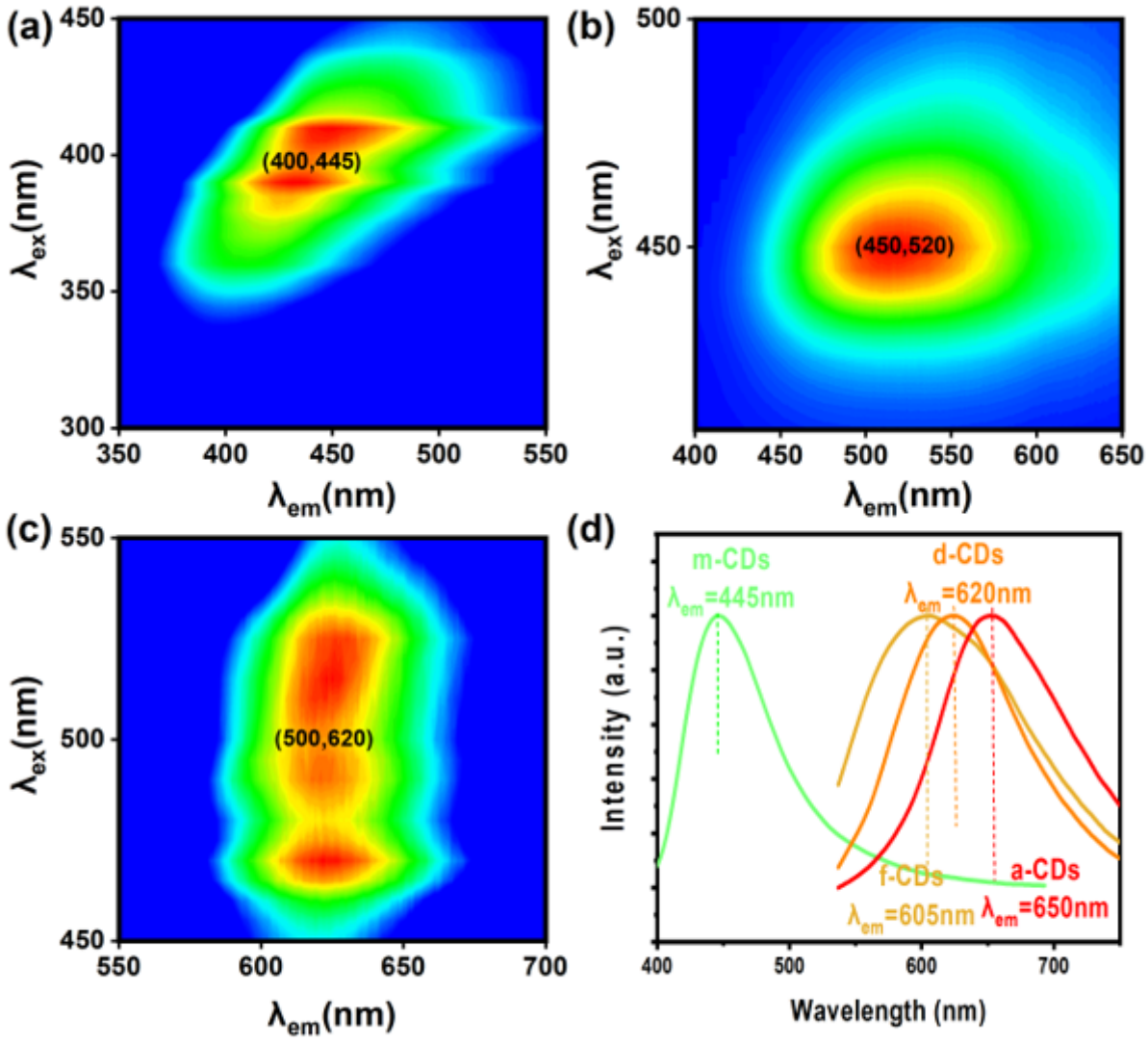

Figure 5

Excitation-emission maps of **(a)** m-CDs **(b)**e-CDs **(c)** d-CDs, **(d)** Normalized fluorescence emission diagram of m-CDs, f-CDs, d-CDs, a-CDs.

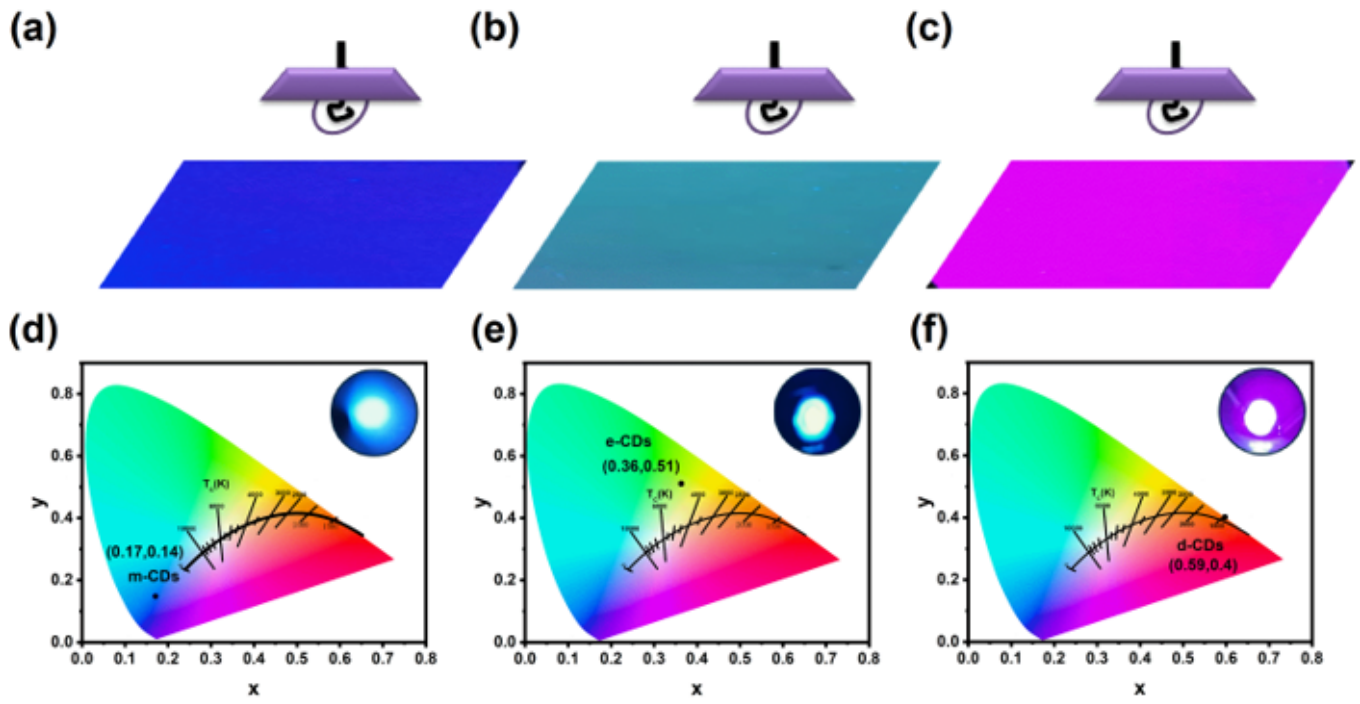

Figure 6

(a) m-CDs@PVP, **(b)**e-CDs@PVP, **(c)** d-CDs@PVP fluorescent film under 365 nm excitation, the corresponding CIE color coordinates of the **(d)** m-CDs@PVP, **(e)**e-CDs@PVP, **(f)** d-CDs@PVP based LEDs.

Supplementary Files

This is a list of supplementary files associated with this preprint. Click to download.

- Supplementaryinformation20221105.docx